International Conference on Space Optics—ICSO 2012

Ajaccio, Corse

9–12 October 2012

Edited by Bruno Cugny, Errico Armandillo, and Nikos Karafolas

Preliminary error budget analysis of the coronagraphic instrument metis for the solar orbiter ESA mission

Vania Da Deppo

Luca Poletto

Giuseppe Crescenzio

Silvano Fineschi

et al.

International Conference on Space Optics — ICSO 2012, edited by Bruno Cugny, Errico Armandillo, Nikos Karafolas
Proc. of SPIE Vol. 10564, 105643B · © 2012 ESA and CNES · CCC code: 0277-786X/17/$18 · doi: 10.1117/12.2309067

Preliminary error budget analysis of the coronagraphic instrument METIS for the Solar Orbiter ESA mission

Vania Da Deppo, Luca Poletto
CNR - Istituto di Fotonica e Nanotecnologie
Padova, Italy
vania.dadeppo@ifn.cnr.it

Giuseppe Crescenzio, Silvano Fineschi, Ester Antonucci
INAF - Osservatorio Astronomico di Torino
Torino, Italy

Giampiero Naletto
University of Padova
Department of Information Engineering and CISAS
Padova, Italy

***Abstract* — METIS, the Multi Element Telescope for Imaging and Spectroscopy, is the solar coronagraph foreseen for the ESA Solar Orbiter mission. METIS is conceived to image the solar corona from a near-Sun orbit in three different spectral bands: in the HeII EUV narrow band at 30.4 nm, in the HI UV narrow band at 121.6 nm, and in the polarized visible light band (590 – 650 nm). It also incorporates the capability of multi-slit spectroscopy of the corona in the UV/EUV range at different heliocentric heights.**

METIS is an externally occulted coronagraph which adopts an "inverted occulted" configuration. The Inverted external occulter (IEO) is a small circular aperture at the METIS entrance; the Sun-disk light is rejected by a spherical mirror M0 through the same aperture, while the coronal light is collected by two annular mirrors M1-M2 realizing a Gregorian telescope. To allocate the spectroscopic part, one portion of the M2 is covered by a grating (i.e. approximately 1/8 of the solar corona will not be imaged).

This paper presents the error budget analysis for this new-concept coronagraph configuration, which incorporates 3 different sub-channels: UV and EUV imaging sub-channel, in which the UV and EUV light paths have in common the detector and all of the optical elements but a filter, the polarimetric visible light sub-channel which, after the telescope optics, has a dedicated relay optics and a polarizing unit, and the spectroscopic sub-channel, which shares the filters and the detector with the UV-EUV imaging one, but includes a grating instead of the secondary mirror.

The tolerance analysis of such an instrument is quite complex: in fact not only the optical performance for the 3 sub-channels has to be maintained simultaneously, but also the positions of M0 and of the occulters (IEO, internal occulter and Lyot stop), which guarantee the optimal disk light suppression, have to be taken into account as tolerancing parameters.

In the aim of assuring the scientific requirements are optimally fulfilled for all the sub-channels, the preliminary results of manufacturing, alignment and stability tolerance analysis for the whole instrument will be described and discussed.

Keywords: coronagraphy; tolerance analysis; optical simulation and performance prediction; imaging and spectroscopy

I. INTRODUCTION

Although over the past decades a major push-forward in the knowledge of the solar corona and its interactions with the heliosphere has been carried out thanks to several space missions (for example Skylab, SOHO, SPARTAN, TRACE, STEREO, and many others), many open questions remain. As a matter of fact, the region in which the heliospheric structures are formed and the solar wind is generated is still not entirely investigated and the physical processes underlying the formation of these structures are not completely known.

The Solar Orbiter (SO) mission [1], foreseen to be launched in 2017, is one of the mission foreseen in the framework of the Cosmic Vision 2015-2025 ESA program. With a combination of in-situ and remote sensing instruments and thanks to its inner heliospheric mission design, SO is conceived for the circumsolar region exploration with the purpose of giving an answer to the scientific questions on how the heliosphere is generated and controlled by the Sun.

The Multi Element Telescope for Imaging and Spectroscopy (METIS) is one of the remote sensing instruments allocated in the SO spacecraft.

The SO designed orbit will bring the spacecraft up to 0.28 AU from the Sun and thus METIS will be able to acquire the first images of the Sun from an out of the ecliptic orbit. Moreover, this specific orbit will allow a quasi-heliosynchronous phase of observation, making possible the investigation of low atmospheric structures, precluded for the near-Earth orbits, the study of the source and acceleration phase of the solar energetic particles, slow and fast solar winds, eruption and early evolution of the coronal mass ejections.

To fulfill all these scientific requirements, METIS [2][3] is conceived to perform both visible and UV/EUV imaging, and UV/EUV spectroscopy of the solar corona.

II. METIS OPTICAL DESIGN AND PERFORMANCE

A. METIS optical design

The METIS instrument is conceived to image the solar corona from a near-Sun orbit in three different spectral bands: the EUV narrow band HeII Lyman-α at 30.4 nm, the UV narrow band HI Lyman-α at 121.6 nm, and the polarized broad-band visible light (590 – 650 nm). It also incorporates the capability of multi-slit spectroscopy of the corona in the UV/EUV range at different heliocentric heights.

The annular Field of View (FoV) covered by METIS telescope ranges between 1.4 and 3.0 solar radii, when the spacecraft is at the perihelion, at 0.28 AU; the attained scale factor is 20 arcsec per pixel.

METIS is an externally occulted coronagraph which adopts an "inverted occulted" configuration [4][5]. The Inverted External Occulter (IEO) is a small circular aperture on the spacecraft Sun facing thermal shield. The disk-light passing through the IEO is rejected back by a spherical heat-rejection mirror (M0). The coronal light, on the other hand, is collected by an on-axis Gregorian telescope. To allocate the spectroscopic part, one portion of the secondary mirror, M2, is covered by a grating (i.e. approximately 1/8 of the solar corona will not be imaged). Fig. 1 shows a schematic layout of the METIS "inverted occulted" coronagraph.

The suppression of the light diffracted off the edges of the IEO and M0 is achieved, respectively, with an Internal Occulter (IO) and a Lyot Stop (LS) [6][7].

METIS consists of a single optical head which incorporates 3 different sub-channels: UV and EUV imaging sub-channel, in which the UV and EUV light paths have in common the detector and all of the optical elements but a filter; the polarimetric Visible Light (VL) sub-channel which, after the telescope optics, has a dedicated relay optics and a polarizing unit; and the spectroscopic sub-channel, which shares the filters and the detector with the UV-EUV imaging one, but includes a grating instead of the secondary mirror.

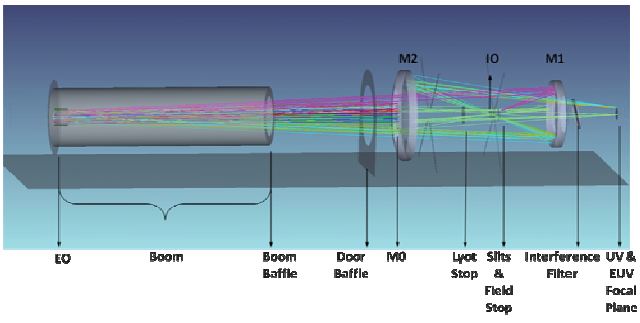

Fig. 1. METIS telescope layout.

B. UV/EUV and Visible-light imaging paths

The coronal light gathered by the METIS Gregorian telescope is divided in the different UV, EUV and VL paths through the filters mounted on a filter wheel mechanism. The filter wheel is inclined at 12° with respect to the telescope optical axis and it is inserted in the converging beam exiting the M2 mirror. The filter wheel hosts:

- an Aluminum thin filter that selects the EUV 30.4 nm line;
- an interference ($Al+MgF_2$) filter that reflects the VL and transmits the UV 121.6 nm.

The primary (M1) and secondary (M2) telescope mirrors are coated with multilayer (ML) coatings which are optimized to enhance the reflectivity for the narrow bandpass at 30.4 nm [8]; those ML coatings have good reflectivity also in the UV and visible-light bands [9].

Inside the polarimetric path [10], see Fig. 2, a broad band filter selects the VL bandpass (590-650 nm). The VL polarimeter sub-channel includes a polarization modulation package (PMP) with a liquid crystal variable retarder (LCVR) [11] together with a fixed quarter-wave retarder and a linear polarizer in "Senarmont" configuration. The PMP is placed in-between a relay optics system that collimates, through the PMP, the linearly polarized VL from the K-corona and refocuses it on the VL detector.

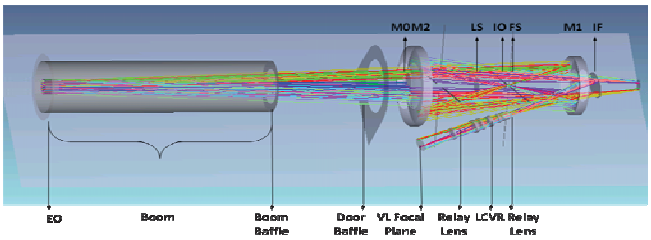

Fig. 2. METIS VL polarimetric path layout.

C. Spectroscopic path

The METIS spectroscopic path is shown in Fig. 3. It is obtained through the insertion of two optical elements: a multi-slit block in the focal plane of M1 and a grating in front of M2 [12].

The slit block is composed by three slits positioned at 1.5°, 1.8°, 2.1° FoV; the grating is a spherical varied line-spaced (SVLS) diffraction grating which diffracts the HI 121.6 nm line at 1st order and the HeII 30. 4 nm line at the 4th order.

Concerning the optical performance at least 50% of the energy is enclosed within 2 pixels for each of the slit in the direction of the spectral dispersion. With regards to the spatial resolution, it is limited for each of the slit respectively to 2, 3, 4 pixels.

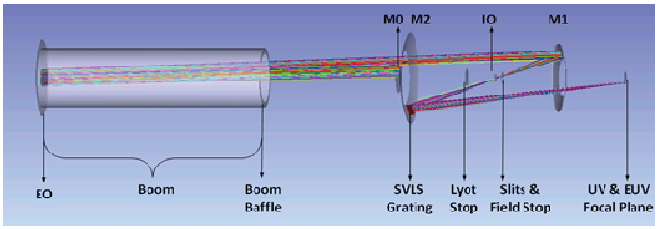

Fig. 3. METIS spectroscopic path layout.

A summary of the METIS instrument characteristics and performance are presented in TABLE I.

The estimated optical performance of the EUV, UV and VL path, including the diffraction effect, is shown in Fig. 4.

TABLE I. SUMMARY OF METIS INSTRUMENT CHARACTERISTICS

METIS instrument performance	
Coronal Imaging	
Wavelength range	VL: 590-650 nm UV: 121.6 ± 10 nm EUV: 30.4 ± 2 nm
Spatial resolution	VL: 10 arcsec/px UV/EUV: 20 arcsec/px
FoV	1.5°-2.9°
Avarage Straylight (B_{cor}/B_{sun})	VL< 10^{-9} UV/EUV< 10^{-7}
Coronal Spectroscopy	
Wavelength range	UV: 121.6 ± 0.9 nm EUV: 30.4 ± 0.22 nm
Spectral resolution	UV: 0.072 nm EUV: 0.018 nm
Spatial resolution	45 arcsec/px
FoV	Slit radial positions: 1.5°, 1.8°, 2.1° Slit extension: 0.8°
Detectors	
Detector	VL: 2048x2048 18 µm pixel UV/EUV: 1024x1024 30 µm pixel

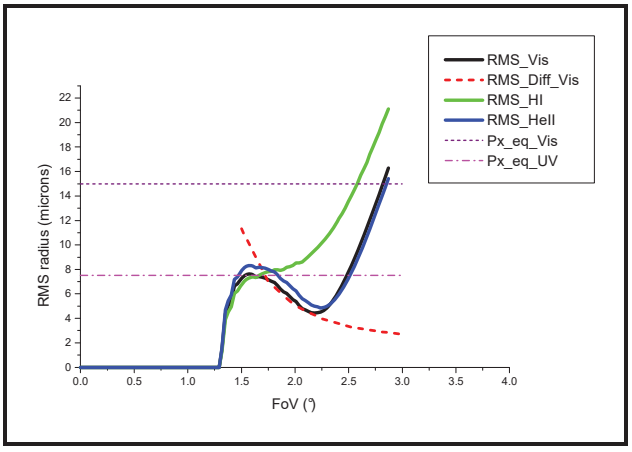

Fig. 4. METIS telescope performance.

III. ERROR BUDGET ANALYSIS

The aim of the error budget analysis is to estimate the optical 'manufacturing and alignment' tolerance, the optical quality stability tolerance over the whole mission lifetime (long term stability), and that over the time of one (or 4, for the VL path) image acquisition (short term stability).

The tolerance analysis has been done taking into account that METIS has 3 different sub-channels and that the telescope mirrors (M1 and M2) are in common to both the UV/EUV and the VL path. Moreover the interference filter is in common for the UV and VL channel. So the tolerance analysis has to consider the degradation of all the configurations at the same time.

For a coronagraphic instrument the straylight issue is extremely important, so the tolerance process has also to pay attention to the impact of the tolerance on the straylight suppression level.

For the UV/EUV and VL path, the figure of merit considered for the 'manufacturing and alignment' and the long term stability tolerance analysis is the rms spot radius. A degradation of 30% of the rms radius has been considered in both cases, thus accepting a global 40% degradation in total (quadratic sum).

For the short term stability tolerance analysis, the boresight error has been taken as the figure of merit and a shift of about 1 px has been considered as the maximum acceptable degradation.

As the imaging of the internal parts of the corona is the most interesting part for the scientific analysis, the internal fields have been weighted more than the external ones in the tolerance analysis process.

The tolerance analysis for the VL and spectroscopic path has been divided in two steps, the tolerance analysis of the telescope unit is done per se, then the VL and spectroscopic path are considered as two independent modules.

A. Telescope Error Budget

The telescope tolerance analysis has been done at the focus of the UV/EUV configuration and at the intermediate focus of the VL configuration, i.e. the telescope focus.

In TABLE II the 'manufacturing and alignment' tolerances are reported; the manufacturing tolerance includes also the effect due to the element mountings (for example the deformation induced on the mirror surface due to its mounting).

The long term and short term tolerances are reported respectively in TABLE III and TABLE IV.

For the alignment and integration phase, the position of the detector has been considered as a compensator, while for the VL path, the position of the whole polarimetric module has been considered as a compensator.

As for the filter, the tolerance analysis considers both the tolerance on the positioning of the filter inside the filter wheel frame (F) and the tolerance on the position of the whole filter wheel frame (FWF).

TABLE II. TELESCOPE MANUFACTURING AND ALIGNMENT TOLERANCE

Telescope Manufacturing and Alignment tolerance	
Mirror tolerance	
$\Delta R_{M1/M2}$	0.2 mm
$\Delta k_{M1/M2}$	0.004/0.001
Δd_{M1-M2}	0.15 mm
$\Delta dec_{M1/M2}$	0.04 mm
$\Delta tilt_{M1/M2}$	0.01°
Filter tolerance	
$\Delta R_{F1/F2}$	5 λ/10 mm
$\Delta d_{F1/F2}$	0.1 mm
$\Delta dec_{F1/F2}$	0.2 mm
$\Delta tilt_{F1/F2}$	0.2°
$\Delta dec_{F/FWF}$	0.1 mm
$\Delta tilt_{F/FWF}$	0.1°
Detector tolerance	
Δtilt	0.5°
Compensators	
Detector position	VL: ± 1.5 mm (z), ± 1 mm (x,y) UV/EUV: ± 1 mm (z)

TABLE III. TELESCOPE LONG TERM STABILITY TOLERANCE

Long term stability	
Mirror tolerance	
$\Delta R_{M1/M2}$	35/15 µm
$\Delta k_{M1/M2}$	0.003/0.001
Δd_{M1-M2}	15 µm
$\Delta dec_{M1/M2}$	0.04 mm
$\Delta tilt_{M1/M2}$	0.01°
Filter tolerance	
$\Delta R_{F1/F2}$	5 λ/10 mm
$\Delta d_{F1/F2}$	0.05 mm
$\Delta dec_{F1/F2}$	0.2 mm
$\Delta tilt_{F1/F2}$	0.15°
$\Delta dec_{F/FWF}$	30 µm
$\Delta tilt_{F/FWF}$	0.04°
Detector tolerance	
Δtilt	0.35°
Δd	50 µm

TABLE IV. TELESCOPE SHORT TERM STABILITY TOLERANCE

Short term stability			
	EUV	**UV**	**VL (4 exp)**
Mirror tolerance			
$\Delta dec_{M1/M2}$ $\Delta tilt_{M1/M2}$	4/2.8 µm 3/1.8 arcsec	2.7/1.9 µm 2/1 arcsec	1.4/0.9 µm 1/0.6 arcsec
Filter tolerance			
$\Delta dec_{F/FWF}$ $\Delta tilt_{F/FWF}$		- 0.05°	7 µm 3 arcsec
Detector tolerance			
Δdec	9 µm	6 µm	3 µm

B. Visible Light path

VL path tolerances analysis is divided in two parts: element analysis (i.e. decenter and tilt of the lenses/doublets) and surfaces analysis (i.e. decenter and tilt of each lens/doublet surface).

The results of the analysis are summarized in TABLE V; where the tolerances have been divided considering the optical elements composing the relay collimating optics and the PMP: the first collimating doublet (D_{in}), the PMP itself, the out doublet (D_{out}) and the focusing lens (FL).

TABLE V. VL PATH TOLERANCE

VL tolerance			
	Man&Align	**Long Stab**	**Short Stab**
Doublet-in (Din) tolerance			
$\Delta R_{Din1/2/3}$	0.4/0.16/0.4 mm	100/8/36 µm	100/8/36 µm
Δdec_{Din}	0.4 mm	0.4 mm	0.2 mm
$\Delta tilt_{Din}$	0.4°	0.4°	0.2°
$\Delta dec_{Din1/2/3}$	0.12/0.11/0.4 mm	0.11/0.11/0.2 mm	2/35/5 µm
$\Delta tilt_{Din1/2/3}$	0.08/0.15/0.4 °	0.08/0.15/0.2 °	7/18/10 arcsec
Polarimeter element tolerance			
Δdec	0.4 mm	0.2 mm	0.2 mm
Δtilt	0.4°	0.2°	0.2°
Δdec_{surf}	0.4 mm	0.2 mm	0.2 mm
$\Delta tilt_{surf}$	0.4	0.2°	10 arcsec
Doublet-out (Dout) & focusing lens (FL) tolerance			
$\Delta R_{Dout1/2/3}$	0.1/0.4/0.4 mm	0.062/0.2/0.1 mm	0.062/0.2/0.1 mm
Δdec_{Dout}	0.07 mm	0.003 mm	0.003 mm
$\Delta tilt_{Dout}$	0.1°	0.1°	0.1°
$\Delta dec_{Dout1/2/3}$	0.07/0.4/0.4 mm	0.06/0.2/0.2 mm	2/70/7 µm
$\Delta tilt_{Dout1/2/3}$	0.07/0.07/0.14 °	0.2°	10/18/6 arcsec
$\Delta R_{FL1/2}$	0.4/0.4 mm	0.2/0.2 mm	0.2/0.2 mm
Δdec_{FL}	0.08 mm	0.05 mm	0.05 mm
$\Delta tilt_{FL}$	0.4°	0.1°	0.1°
$\Delta dec_{FL1/2}$	0.07/0.4 mm	0.07/0.2 mm	16/23 µm
$\Delta tilt_{FL1/2}$	0.4°	0.2°	16 arcsec

C. Spectroscopic path

The characteristic and performance of the spectroscopic path are different from those of the imaging paths, so a different acceptable degradation has been considered.

In particular, the tolerances corresponding to a maximum acceptable degradation of 50% (encircled energy) along the spectral direction, and to a decrease of 20% of the flux passing through the first inner slit have been calculated. Also, it has been assumed a possible error of 1% in the grating radius of curvature.

The spectrum is shifted by 0.25 mm, equivalent to 10 px, if the grating is rotated by 1 arcmin in x or y and by 10 arcmin in z (for the axes orientation see Fig. 5).

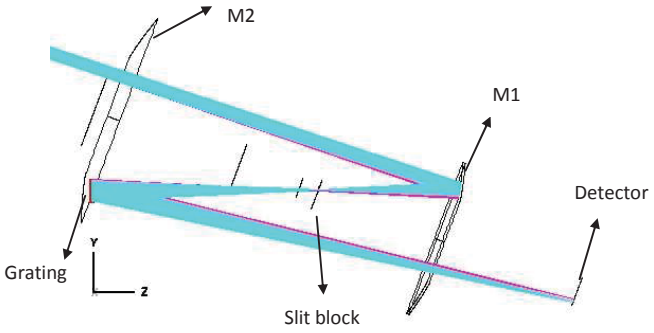

Fig. 5. Detail of the spectroscopic path with the adopted reference system.

The tolerance analysis for the spectrometer path includes also the position tolerance analysis of the slit block.

The spectroscopic path tolerances are summarized in the following table (TABLE VI).

TABLE VI. SPECTROSCOPIC PATH TOLERANCE

Spectroscopic path tolerance			
	Grating manufacturing and alignment tolerance	*Grating stability tolerance*	
ΔR Δdec_z $\Delta tilt_x$	1% 1.25 mm 0.02°	$\Delta dec_{z,x,y}$ $\Delta tilt_{x,y,z}$	0.5/1/0.7 mm 1/1/10 arcmin
Slit block tolerance			
Δdec_{slit} $\Delta tilt_{slit}$	0.2/0.1/0.1 mm 2.5/8/4 °		

D. IEO and IO tolerance analysis

The IO and the LS block the diffracted light produced respectively by IEO and M0 edges. Since the IEO and M0 edges are conjugated, via the M1 mirror, with IO and LS, their blocking properties are directly related to the M1 tolerance.

For the LS an appropriate oversizing of the element is sufficient to deal with the problem, considering that the position of this element is not particular affected by M0 shift and M1 rotation. For IO instead, which is more critical, an appropriate mechanism is foreseen to reposition it during the flight.

IO and IEO tolerances for the integration phase on ground and for the stability long term and short term in-flight are summarized in TABLE VII.

TABLE VII. IEO AND IO TOLERANCES ('MANUFACTURING AND ALIGNMENT', LONG AND SHORT TERM STABILITY).

IEO and IO tolerance			
	Man&Int	**Long Stab**	**Short Stab**
Δd_{IEO-M1} Δdec_{IEO}	1 mm 0.3 mm	1 mm 0.3 mm	1 mm 0.03 mm
Δd_{IO-M1} Δdec_{IO}	0.15 mm 0.15 mm	0.15 mm 0.15 mm	0.015 mm 0.005 mm
ΔR_{M1} Δdec_{M1} $\Delta tilt_{M1}$	0.2 mm 0.040 mm 40 arcsec	35 µm 0.04 mm 4 arcsec	35 µm 0.004 mm 3° arcsec
	(*)The highlighted values are those of the parameters used as compensators		

IV. CONCLUSIONS

The preliminary tolerance analysis for the coronagraphic METIS instrument for the ESA Solar Orbiter mission has been presented. The analysis has been done considering the peculiar design of the instrument. METIS comprises in one single unit different sub-channels sharing most of the optical components.

The tolerance analyses for the different phase of the instrument life have been calculated: manufacturing and alignment tolerance for the realization on ground; long term stability tolerance to assure the stability of the performance over the whole mission life time; short term stability tolerance to guarantee the quality and stability of the image during each exposure.

The tolerances have been calculated for each of the optical paths of the instrument: telescope unit, UV/EUV, VL and spectroscopic paths. The manufacturing and alignment tolerances are well within the capabilities of the optical manufacturers, long term and in particular short term stability tolerance for the VL path are instead quite challenging.

For the telescope, the worst offenders during the whole mission lifetime are the curvatures stability of the mirrors and their relative position; for the VL path the stability of the inclination of the interference filter is the major critical point. For the grating the worst offenders are the rotations of the grating, since these movements change the position of the spectrum on the detector.

As for the short term stability over one single exposure, the stability in term of rotation of the mirrors and filter is the major concern.

Being the straylight due to the diffraction on the edges of IEO and M0 mirror an issue for this kind of instrument, a discussion on the tolerance analysis for the IO and LS stop has also been given.

ACKNOWLEDGMENT

This activity has been realized under the "Solar Orbiter" Agenzia Spaziale Italiana (ASI) contract to the Istituto Nazionale di Astrofisica (INAF) I/013/12/0.

REFERENCES

[1] D. Muller, R. G. Marsden, O. C. StCyr, H. R. Gilbert, "Solar Orbiter: Exploring the Sun-heliosphere connection", Solar Physics, in press.

[2] Naletto et al., "METIS, the Multi Element Telescope for Imaging and Spectroscopy for the Solar Orbiter mission", Proc. ICSO 2010 – Rhodes, 2010.

[3] E. Antonucci et al., "Multi Element Telescope for Imaging and Spectroscopy (METIS) coronagraph for the Solar Orbiter Mission", Proc. SPIE 8443, in press.

[4] S. Fineschi, "Novel Optical Designs for Space Coronagraphs: inverted occulters and Lyot-stops", Proc. ICSO 2010 – Rhodes 2010.

[5] S. Fineschi et al., "METIS: a novel coronagraph design for the Solar Orbiter mission", Proc. SPIE 8443, in press.

[6] F. Landini et al., "Optimization of the occulter for the Solar Orbiter/METIS coronagraph", Proc. SPIE 8442, in press.

[7] E. Verroi, V. Da Deppo, G. Naletto, S. Fineschi, E. Antonucci, "Preliminary internal straylight analysis of the METIS instrument fo the Solar Orbiter ESA mission", Proc. SPIE 8442, in press.

[8] M.-G. Pelizzo, D. Gardiol, P. Nicolosi, A. Patelli, V. Rigato, "Design, deposition, and characterization of multilayer coatings for the Ultraviolet and Visible-Light Coronagraphic Imager", App. Optics, vol. 43(13), pp. 2661-2669, 2004.

[9] A. J. Corso, P. Zuppella, P. Nicolosi, D. L. Windt, E. Gullikson, M.-G. Pelizzo, "Capped Mo/Si multilayers with improved performance at 30.4 nm for future solar missions", Optics Express, vol. 19(15), pp. 13963-13973, 2011.

[10] G. Crescenzio et al., "Imaging polarimetry with the METIS coronagraph of the Solar Orbiter Mission", Proc. SPIE 8443, in press.

[11] G. Capobianco et al., "Electro-optical polarimeters for ground-based and space-based observations of the solar K-corona", Proc. SPIE 8450, in press.

[12] S. Fineschi, C. Korendyke, J. D. Moses, R. T. Thomas, "Solar ultraviolet spectro-coronagraph with toroidal varied line-space (TVLS) grating", Proc. SPIE 5487, p. 1165, 2004.